TNF-17 target flames

Multi scalar Raman-Rayleigh measurements of piloted turbulent homogeneous and inhomogeneous partially premixed H_2/N_2/Air flames

A.R.W. Macfarlane[a, b*], H. Tang[c], M.J. Dunn[a], G. Magnotti[d, e], A.R. Masri[a]

[a]School of Aerospace Mechanical and Mechatronic Engineering, University of Sydney, NSW 2006, Australia
[b]Department of Mechanical Engineering, Reactive Flows and Diagnostics, Technical University of Darmstadt, Otto-Berndt-Str. 3, Darmstadt, 64287, Germany
[c] Daniel Guggenheim School of Aerospace Engineering, Georgia Institute of Technology, Atlanta, GA 30332, USA
[d] Clean Combustion Research, King Abdullah University of Science and Technology (KAUST). Thuwal, 23955-6900. Saudi Arabia
[e]INSA Rouen Normandie and CNRS UMR6614-CORIA, Saint-Étienne-du-Rouvray, 76801, France
*amac7548@uni.sydney.edu.au

Introduction:

The piloted Sydney Inhomogeneous burner is used to generate the turbulent inhomogeneous and homogeneous flames. This burner is now well studied for partially premixed methane flames [1-4] ($\varphi = 4.76$) where the current results are extended to hydrogen flames. The H_2 is further mixed with 60 % N_2 to reduce the homogeneous blow-off velocity and ensure the flow remains incompressible. The burner varies the degree of inhomogeneity and mixedness by recessing a central fuel jet within the annulus containing air. For the previous methane flames there is an optimal position that achieved a local blow-off velocity 50 % greater than the homogeneous velocity, however, for the current measurements only a local plateau in blow-off velocity was observed. The current results showcase large differences between the homogeneous and inhomogeneous flames, particularly for differential diffusion and flame length. The reduction in differential diffusion and the smaller flame length, for the inhomogeneous flame, are believed to be coupled and are attributed to the extreme mixing that occurs with reduced jet recess.

Burner geometry and flame selection

The burner (Figure 1a) consists of three concentric tubes: the outer pilot ($Ø_{Pilot}$ = 13 mm), middle annulus ($Ø_{Annulus}$ = 5.5 mm) and inner fuel tube ($Ø_{Jet}$ = 2.85 mm), where the air is in the annulus and fuel in the jet (Figure 1b, F_J configuration). The annulus diameter is the dimension used for the non-dimensional parameter x/D. The amount of air in the annulus is kept constant throughout and is used to achieve a global equivalence ratio of $\varphi = 4.76$. The annulus issues pure air with the jet containing the fuel (H_2/N_2=40/60). The difference in the diameters between the annulus/air and jet/fuel creates an area ratio of approximately two ($A_{An}/A_J \sim 2$), this is relevant to the velocity ratio between the two streams. The large addition of N_2 to the fuel jet entails that the fuel-to-air ratio increases from two to five, the significantly higher flow rate of fuel compared to the air means that the velocity ratio is 11 ($U_J/U_A = 11$). This velocity ratio dictates the high levels of turbulence with reduced jet recession. For a large recession of $L_r = 300$ the velocity profile is somewhat top hat at the outlet, whilst for minimal recession there is a large degree of shear at the outlet; these velocity profile differences are observed in the paper by Meares et al. [3]. The outer pilot consists of the same $H_2/N_2 = 40/60$ composition as the fuel jet; however, it is at stoichiometric conditions with a power of $\dot{Q}_{Pilot} = 114\ W$. The burner is surrounded by a coflow ($Ø_{Coflow}$ = 250 mm) of air at $U_c = 9$ m.s^{-1}.

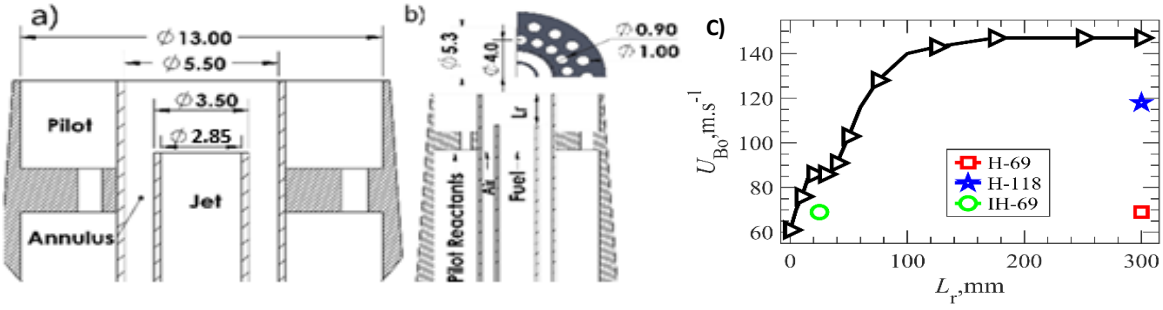

Figure 1 Burner schematic (a) Flow conditions (b) blow-off velocities (c)

For an equivalence ratio of φ = 4.76 and H_2/N_2=40/60, blow-off velocities are generated for each recess position as observed by Figure 1 (c). The inhomogeneous and comparative homogeneous flames are selected to be at 80 % of the blow-off velocity (U_{Bo} = 80 %) since this is known to have significant local extinction and downstream reignition. Therefore, Raman/Rayleigh multiscalar measurements are obtained for the homogeneous flame (L_r = 300) with the velocity being U = 118 m.s^{-1} (H-118, blue star). Similarly, for the inhomogeneous flame (L_r = 25) the blow-off velocity is lower such that the velocity used throughout is U = 69 m.s^{-1} (IH-69, green circle). A second homogeneous flame at U = 69 m.s^{-1} (H-69, red square) is also chosen to have the same velocity as the inhomogeneous flame which has a lower blow-off percentage of U_{Bo} = 58 %. The three flame conditions are listed in Table 1, the names used are for simplification throughout.

Table 1 Flame conditions

Name	L_r, mm	U, m.s^{-1}	U_{Bo}, %	Re	$\dot{Q}_{Pilot}$, W	Φ	U_C, m.s^{-1}
H-69	300	69	58	17,890	114	4.76	9
H-118	300	118	80	30,595	114	4.76	9
IH-69	25	69	80	17,890	114	4.76	9

Global flame Structure

Images for the three flames are given in Figure 2. Figure 2 (a) presents average digital SLR images with an exposure of two seconds (b) presents stacked single shot OH-PLIF images and (c) gives the average OH-PLIF. The notable observations are that the inhomogeneous flame (IH-69) is significantly shorter and the flame intensity for H-118 is greater. The dashed line indicates the positions where multi-scalar Raman/Rayleigh measurements were taken.

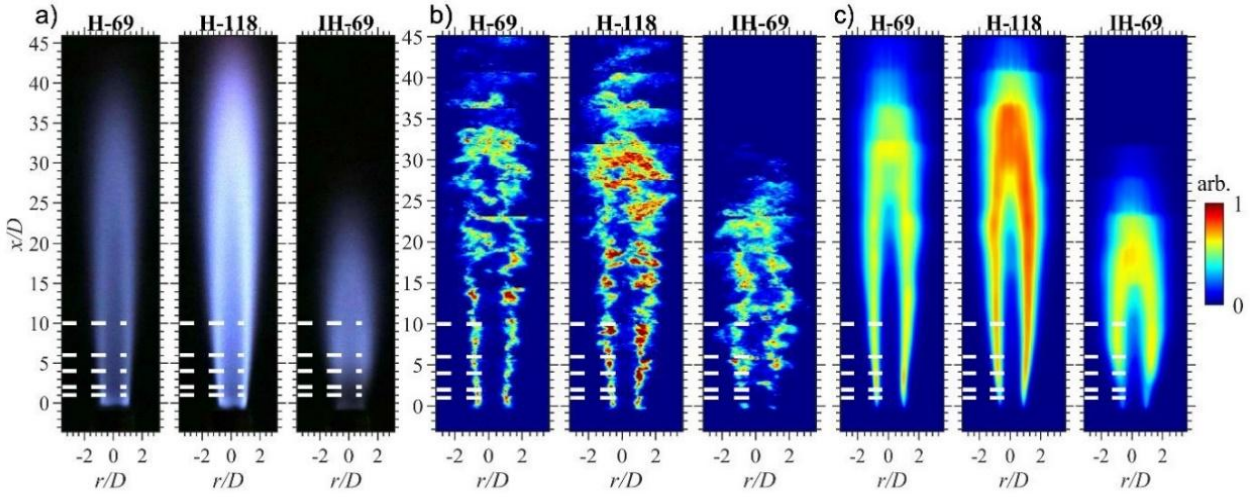

Figure 2 Flame images of all flames: Digital SLR (a), Stacked instantaneous OH-PLIF (b) and average OH-PLIF (c)

Scatter Plots

An extensive data set is now available for the cases listed in Table-1 showing Raman measurements of stable species at various locations within the flames. Such data set will be made available for model development and validation. Figure 3 presents a sample scatter plot of temperature verse the Bilger mixture fraction (ξ) for the three flames studied, for all measured positions (x/D = 1, 2, 4, 6 and 10). It is evident that for IH-69 the scatter is large across all mixture fraction space and the flame rapidly evolves to burn in a diffusive manner by x/D = 10. Near the nozzle the low velocity homogeneous flame (H-69) is like a low strained opposed flow multicomponent diffusion simulation (a = 15 s^{-1}) given by the green dashed line. The high velocity homogeneous flame has a reduced temperature correlated to a higher strain rate with multicomponent diffusion (a = 1000 s^{-1}). IH-69 has the lowest temperature closely related to a unity Lewis simulation (a = 1000 s^{-1}).

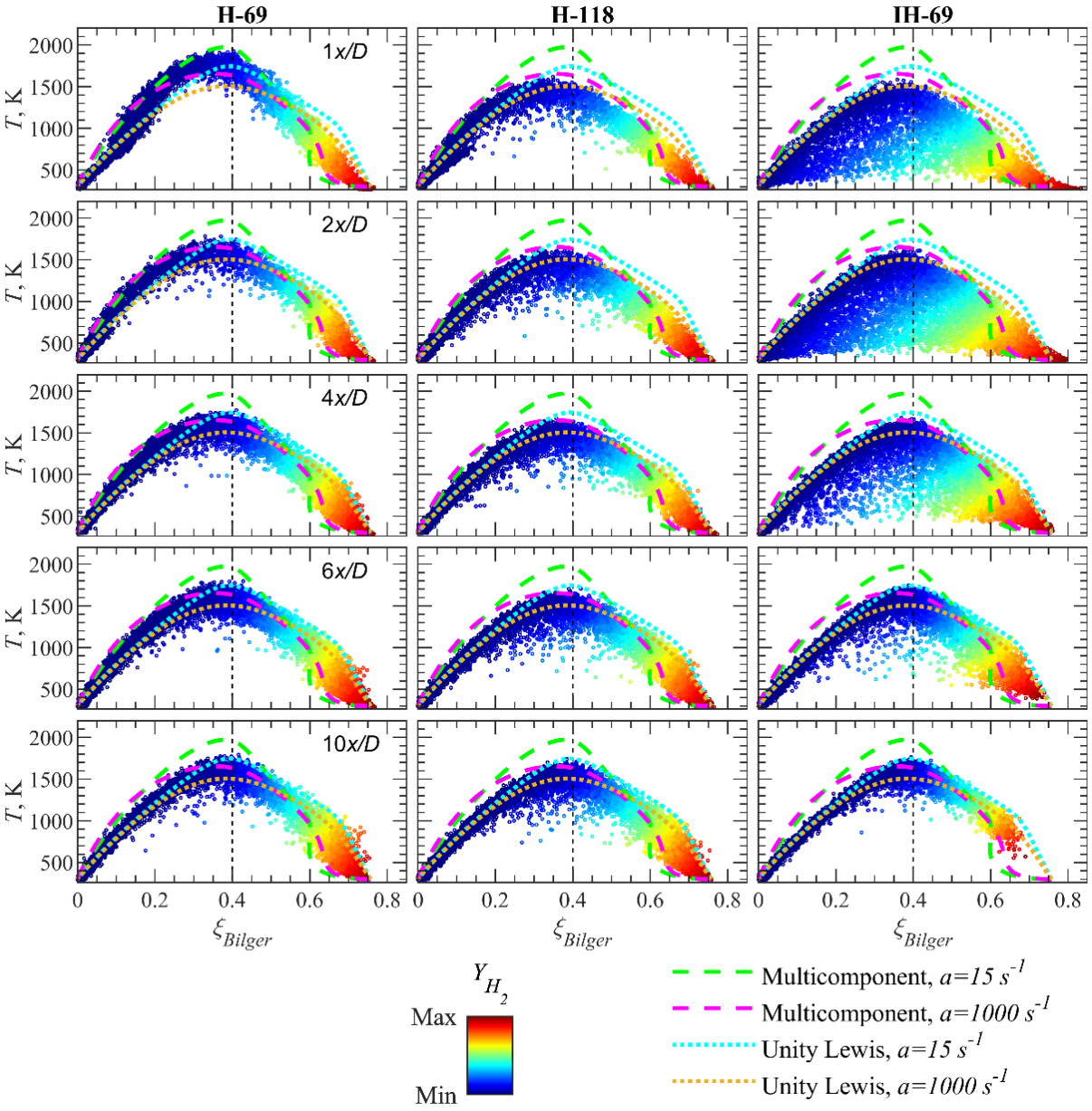

Figure 3 Scatter plots of temperature verse the Bilger mixture fraction for all flames and positions coloured on the hydrogen mass fraction.

References

[1] R.S. Barlow, S. Meares, G. Magnotti, H. Cutcher, A.R. Masri, Local extinction and near-field structure in piloted turbulent CH4/air jet flames with inhomogeneous inlets, Combust. Flame, 162 (2015) 3516-3540.
[2] H.C. Cutcher, R.S. Barlow, G. Magnotti, A.R. Masri, Turbulent flames with compositionally inhomogeneous inlets: Resolved measurements of scalar dissipation rates, Proc. Combust. Inst., 36 (2017) 1737-1745.
[3] S. Meares, A.R. Masri, A modified piloted burner for stabilizing turbulent flames of inhomogeneous mixtures, Combust. Flame, 161 (2014) 484-495.
[4] S. Meares, V.N. Prasad, G. Magnotti, R.S. Barlow, A.R. Masri, Stabilization of piloted turbulent flames with inhomogeneous inlets, Proc. Combust. Inst., 35 (2015) 1477-1484.